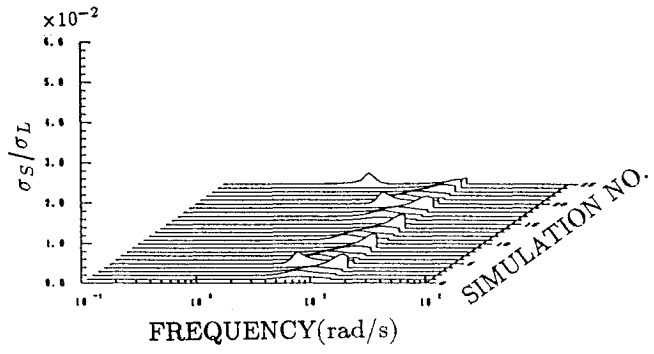

a)

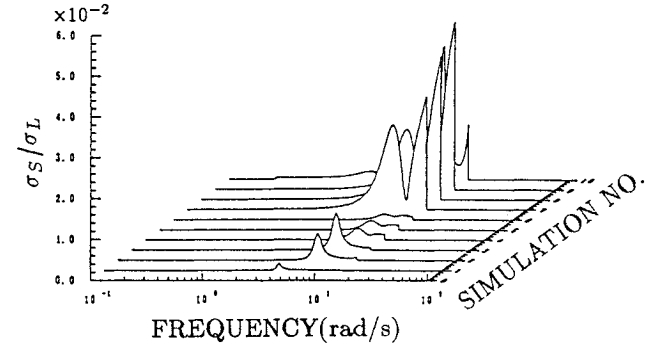

b)

Fig. 4 Results of the singular value analysis: a) D-model simulation, $C_\theta = 0.02$, and b) I-model simulation, $C_\theta = 0.02$.

that for all cases of the D-model simulation the matrix enclosed by a broken line in Eq. (2) is almost singular, suggesting that the D model is the correct structure. On the other hand, Fig. 4b shows that the singular value ratio takes significant values in the frequency range of interest if the inner-loop gain K_{p_θ} is large enough. A close look at Fig. 4b and an analysis can point out the following: a peak exists around the short period mode natural frequency, the peak magnitude increases as the magnitude of Y_{p_h} increases, and the frequency band where the singular value ratio takes significant values shrinks as the pilot remnant intensity increases.

Conclusions

An identification method is proposed to determine the feedback structure employed by the pilot in a system with a choice of feedback structures. The method utilizes an autoregressive scheme and a singular value analysis. The method is applied to an analysis of the computer simulation data of an altitude tracking task. It is shown that the method can make clear judgment on the feedback structure. Application to the data from the real world is to be made in the future.

References

[1]Chalk, C. R., "Flying Qualities of Pitch Rate Command/Attitude Hold Control System for Landing," *Journal of Guidance, Control, and Dynamics*, Vol. 9, No. 5, 1986, pp. 541–545.

[2]Ng, T. S., Goodwin, G. C., and Anderson, B. D. O., "Identifiability of MIMO Linear Dynamic Systems Operating in Closed Loop," *Automatica*, Vol. 13, 1977, pp. 477–485.

[3]Goto, N., and Matsuo, T., "Identification of Pilot Dynamics in a System with a Choice of Feedback Structures," *Journal of Guidance, Control, and Dynamics*, Vol. 11, No. 2, 1988, pp. 159–166.

[4]Stengel, R. F., *Stochastic Optimal Control—Theory and Application*, Wiley, New York, 1986, pp. 591–595

[5]Teper, G. L., "Aircraft Stability and Control Data," STI Tech. Rept. 176-1, Systems Technology, Hawthorne, CA, 1969, pp. 93–103.

Dynamics and Control of Slewing Active Beam

Moon K. Kwak,* Keith K. Denoyer,† and Dino Sciulli‡
Phillips Laboratory, Kirtland Air Force Base, New Mexico 87117

I. Introduction

THE performance requirements of future space systems have brought much attention to the study of the simultaneous slewing and vibration suppression of space structures. To fulfill the requirements of precision spacecraft, the aerospace community has been looking for active structures, i.e., structures with highly integrated sensors and actuators, which can be used to change the mechanical properties of the structure.[1–5]

In this Note, a slewing flexible beam equipped with a multitude of piezoelectric sensox xxrs and actuators is modeled by use of the extended Hamilton principle, resulting in the equations of motion as well as the measurement equations. Nonlinearity enters into the equations of motion through the rigid-body rotational motion, whereas the elastic vibration is assumed to be small compared to the rigid-body rotation. Based on these equations, the decentralized control concept is proposed, which divides controls into the slewing and vibration suppression control. Slewing is achieved by utilizing sliding-mode control[6] as if the system were rigid and the vibration suppression is carried out independently by means of modal-space positive-position-feedback control[7] plus disturbance counteracting control.

All the developments in this paper are verified by the experiment.

II. Modeling of Slewing Active Beam

The motion of the beam is constrained to a horizontal plane and the beam is thin compared to its length so that we can regard it as an Euler-Bernoulli beam. Placed on the beam are piezoceramic plates that can be used as sensors or actuators. To model such a beam, we need to combine the stress-strain relationship of the Euler-Bernoulli beam theory with the piezoelectric constitutive equation. The control design for the hybrid equation is not feasible, so that the elastic displacement is discretized by introducing the admissible functions

$$v = v(x,t) = \sum_{j=1}^{n} \phi_j(x) q_j(t) = \Phi \boldsymbol{q} \tag{1}$$

where $v(x,t)$ is the elastic displacement of the beam, $\Phi = [\phi_1 \ \phi_2 \ldots \phi_n]$ is a vector of assumed mode shape, $\boldsymbol{q} = [q_1 \ q_2 \ldots q_n \ ]^T$ are generalized coordinates, and n is the number of assumed modes, respectively. We assume that the admissible function introduced in Eq. (1) automatically satisfies the boundary conditions. Thus, the total kinetic energy can then be written as

$$T = \tfrac{1}{2} J \dot{\theta}^2 + \tfrac{1}{2} \dot{\theta}^2 \boldsymbol{q}^T M \boldsymbol{q} + \dot{\theta} \tilde{\Phi} \dot{\boldsymbol{q}} + \tfrac{1}{2} \dot{\boldsymbol{q}}^T M \dot{\boldsymbol{q}} \tag{2}$$

where θ is the slewing angle, J is the total mass moment of inertia, M is the total mass matrix, $\tilde{\Phi} = \int \bar{m} x \Phi \, dx$ in which $\bar{m}$ is the mass density, respectively. In addition, the total virtual work has the form

$$\delta W = \delta \boldsymbol{v}^T C \boldsymbol{v} - \delta \boldsymbol{v}^T B^T \boldsymbol{q} - \delta \boldsymbol{q}^T B \boldsymbol{v} - \delta \boldsymbol{q}^T K \boldsymbol{q} + T_h \, \delta\theta \tag{3}$$

where $\boldsymbol{v}$ is the voltage applied or generated in the piezoceramic plate, B and C are coefficient matrices resulting from the piezoelectric property of the piezoceramic plates, K is the total stiffness

Received June 3, 1993; revision received April 19, 1994; accepted for publication April 20, 1994. This paper is declared a work of the U.S. Government and is not subject to copyright protection in the United States.

*Research Assistant Professor, Department of Mechanical Engineering, University of New Mexico. Member AIAA.

†Mechanical Engineer, Structures and Control Division.

‡Aerospace Engineer, Structures and Control Division. Member AIAA.

matrix, and T_h is the torque applied to the hub, respectively. Applying Hamilton's principle with Eqs. (2) and (3) yields the equations of motion. Since some of the piezoceramic plates will be used as actuators and the rest of them will be used as sensors, B and C matrices are divided into the actuator and sensor parts. Also, we need to include gain matrices since the pre- and post-hardware components of the control law are the charge amplifier and the voltage driver. Moreover, the solution of the premaneuver eigenvalue problem for the clamped boundary condition leads to eigenvalues and eigenvectors that satisfy the orthonormality conditions $U^T M U = I, U^T K U = \Lambda$. Thus, including gains and introducing $\boldsymbol{q} = U\boldsymbol{\eta}$, we can obtain

$$\begin{aligned} J\ddot{\theta} + \tilde{\Phi} U\ddot{\boldsymbol{\eta}} &= T_h, \\ U^T\tilde{\Phi}^T\ddot{\theta} + \ddot{\boldsymbol{\eta}} + (\Lambda - \dot{\theta}^2 I)\boldsymbol{\eta} &= -U^T B_a G_a \boldsymbol{v}_a \end{aligned} \tag{4}$$

$$\boldsymbol{v}_s = G_s C_s^{-1} B_s^T U\boldsymbol{\eta} \tag{5}$$

where B_a is an $n \times n_a$ matrix, B_s is an $n \times n_s$ matrix, C_s is an $n_s \times n_s$ matrix, G_a and G_s are the gain matrices of the voltage driver and the charge amplifier in which the dynamics of each circuit is neglected, n_a is the number of actuator sources, and n_s is the number of sensor sources. Note that Eqs. (4) represent the coupled rigid-body rotational motion and the elastic vibration and Eq. (5) represents the sensor equation.

The DC motor drives the active beam. However, the motor torque is not the same as the terminal torque at the hub of the beam. Therefore we need to consider the dynamics of the DC motor. The mathematical model for the DC motor used for the slewing of the beam includes the mass moment of inertia, viscous and Coulomb damping, and static friction. Thus, the equation of motion for the motor is given as

$$J_m\ddot{\theta} + C_v\dot{\theta} + C_c\,\mathrm{sgn}(\dot{\theta}) = r(T_m - T_f) - T_h \tag{6}$$

where J_m is the mass moment of inertia of the motor, C_v represents the viscous damping coefficient of the motor, C_c represents the Coulomb friction of the motor, r is the gear reduction ratio, $T_m = K_T(\alpha_m v_m + \beta_m)$ is the motor torque, T_h is the torque supplied to the hub, T_f represents the static friction torque of the motor, sgn is a sign function, K_T is the motor constant, α_m and β_m are the constant and bias of the servo amplifier, and v_m is the input voltage to the servo amplifier.

Then, using Eqs. (4–6), we can construct the state equation and the measurement equation

$$\dot{\boldsymbol{x}} = \mathcal{A}\boldsymbol{x} + \mathcal{B}\boldsymbol{f} + \boldsymbol{d}, \qquad \boldsymbol{y} = \mathcal{C}\boldsymbol{x} \tag{7}$$

where $\boldsymbol{x} = [\theta\ \boldsymbol{\eta}^T\ \dot{\theta}\ \dot{\boldsymbol{\eta}}^T]^T$ and $\boldsymbol{y} = [\theta\ \dot{\theta}\ \boldsymbol{v}_s^T]^T$.

III. Decentralized Control Design for Slewing and Vibration Suppression

The control objectives are to drive the arm to a certain position as fast as possible with a minimum line-of-sight error, so that vibrations excited by the slewing need to be suppressed simultaneously based on sensor measurements. The equations of motion for the slewing active beam are nonlinear, as can be seen in Eqs. (4). It is worthwhile to note that the experimental results show that uncertainty exists in the system to some extent, the gear box causes unsteady frictions that cannot be modeled properly, and the friction force is so large that the elastic motion cannot disturb the slewing motion. This is in contrast to the assumption that we made in the theory of coupled rigid-flexible motion. In view of this, it seems reasonable to separate the equations of motion for control design, resulting in a decentralized control design.

The control problem is to get the angular displacement θ to track a specific path $\bar{\theta}$ in the presence of the disturbance d_m. To this end, we designed sliding-mode control, which has the form

$$v_m = \frac{1}{b_m}\left[\ddot{\bar{\theta}} + c_m\dot{\bar{\theta}} - \hat{d}_m - g_m\,\mathrm{sgn}(s)\right] \tag{8}$$

where $b_m = rK_T\alpha_m/(J + J_m)$, $c_m = C_v/(J + J_m)$, $\hat{d}_m$ is the estimate of the disturbance, and g_m is the gain, which satisfy the sliding condition.

Although the input voltage applied to the servo motor amplifier is controlled by means of the sliding-mode control law to track the specified path, the piezoceramic actuators are responsible for suppressing vibrations. As can be seen in Eqs. (4), the elastic motions are coupled with the inertia force due to the angular acceleration of the body, which can be regarded as a disturbance to the elastic motion. In view of this, we may divide the vibration suppression control into the disturbance-counteracting control, linearization control, and the regulator, which is in fact the positive position feedback (PPF) control.[7] The advantage of using the PPF control is that we can tune the controller to the natural frequency of interest, thus suppressing that mode individually. Of course, the natural frequencies should be known accurately in advance and also be well separated. Thus, the total control force applied to the beam is

$$\boldsymbol{v}_a = G_a^{-1}B_a^{\dagger}\left(\ddot{\bar{\theta}}\tilde{\Phi}^T - \ddot{\tilde{\theta}}UM\boldsymbol{\eta}\right) + \left(U^T B_a G_a\right)^{\dagger}\boldsymbol{f} \tag{9}$$

where $\boldsymbol{\eta} = (G_s C_s^{-1} B_s^T U)^{\dagger}\boldsymbol{v}_s$ and $\boldsymbol{f} = [f_1\ \ f_2 \cdots f_{n_a}]^T$ is the vector of PPF control forces, which have the form

$$\ddot{f}_i + c_i\dot{f}_i + \lambda_i f_i = g_i\eta_i, \qquad i = 1, 2, \ldots, n_a \tag{10}$$

where c_i is the damping coefficient of the controller and g_i is the gain. In writing Eq. (9), $\ddot{\tilde{\theta}}$ and $\dot{\tilde{\theta}}$ are used instead of $\ddot{\theta}$ and $\dot{\theta}$ because actual sensor signals contain noise. It can be said that the resulting control counteracts the estimated disturbances, linearizes time-varying properties, and at the same time suppresses residual vibrations.

IV. Experiments

The ISI AC-100 data acquisition controller is used in the experiment with the real-time monitor software. Figure 1 shows the test article, in which the motion is constrained to horizontal motion on a 14 × 14-ft-sq granite table. The DC motor is fixed at the center of the granite table, so that the flexible arm can be rotated. Sensors for the experiment include the encoder and piezoceramic sensors. Actuators for the experiment include the PMI DC motor and piezoceramic actuators. Three piezoceramic actuators and three sensors are attached to the beam, where each actuator consists of four piezoceramic plates and each sensor is a small rectangular piece of the piezoceramic plate located between actuators, as shown in Fig. 1. A tip mass has been added to lower the natural frequencies.

The sliding-mode control is applied to the slewing control of the DC motor. The effect of beam flexibility and tip mass on the motion of the DC motor is not noticeable, so that the validity of the decentralized control concept is validated. Figure 2 shows the encoder output of the DC motor and the desired path. As shown in Fig. 2, the sliding-mode control results in chattering behavior, which in turn excites higher modes of the system. The chattering behavior is also observed when applying smooth control voltage into the servo amplifier. This is due to the gear box noise, backlash, and friction. The chattering becomes worse in the case of sliding-mode control. However, the slewing angle exactly follows the desired path. Figure 3 shows the uncontrolled and controlled responses of the piezoceramic sensor under the slewing control. Three admissible functions are considered for control design. It is shown in Fig. 3 that the vibration suppression is achieved and the vibrational amplitude is decreased. However, higher-modes excited during slewing were uncontrollable. It should be noted here that, in applying the control

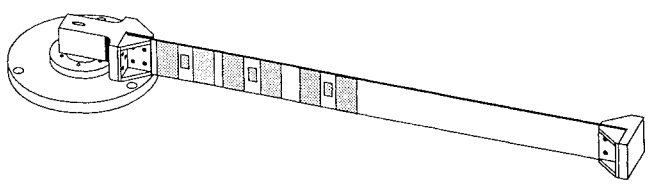

Fig. 1 Slewing active beam experiment.

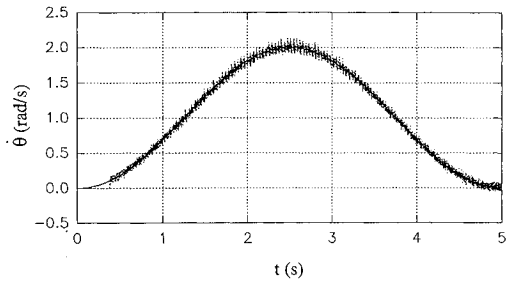

Fig. 2 Controlled elastic response.

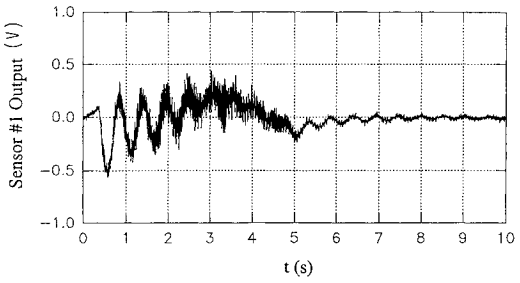

Fig. 3 Time history of angular velocity.

law [Eq. (9)], the disturbance counteracting control part is tuned manually to achieve best performance.

V. Summary and Conclusions

In this Note, the equations of motion are derived for the slewing active beam equipped with multitudes of piezoelectric sensors and actuators by means of the extended Hamilton principle. Based on these equations of motion, a decentralized control technique is proposed to meet the mission requirement. Hence, controls are divided into the slewing control and the vibration suppression controls. The sliding-mode control is proposed as the slewing control and the modal-space positive position feedback plus disturbance-counteracting control is developed for the suppression of vibrations.

The developed control techniques are applied to the testbed and verified by the experiment. The experimental results show that the decentralized controls performed satisfactorily but high-frequency vibrations remained uncontrolled. In order to maintain the control authority over these higher modes, more actuators and sensors are needed. In addition, more powerful piezoelectric actuators are desirable.

Acknowledgment

This work is supported in part by the Air Force Office of Scientific Research.

References

[1]Crawley, E. F., and de Luis, J., "Use of Piezoelectric Actuators as Elements of Intelligent Structures," *AIAA Journal*, Vol. 25, No. 10, 1987, pp. 1373–1385.

[2]Hagwood, N. W., Chung, W. H., and von Flotow, A., "Modeling of Piezo Actuator Dynamics for Active Structural Controls," *Journal of Intelligent Material Systems and Structures*, Vol. 1, No. 3, 1990, pp. 327–354.

[3]Garcia, E., and Inman, D. J., "Advantages of Slewing an Active Structure," *Journal of Intelligent Material Systems and Structures*, Vol. 1, 1990, pp. 261–272.

[4]Denoyer, K. K., and Kwak, M. K., "Dynamic Modeling and Vibration Suppression of a Slewing Active Structure Utilizing Piezoelectric Sensors and Actuators," *Proceedings of the SPIE Smart Structures and Materials Conference* (Alburquerque, NM), Vol. 1917, 1993, pp. 882–894.

[5]Kwak, M. K., Denoyer, K. K., and Sciulli, D., "Dynamics and Control of a Slewing Active Beam," paper presented at the Ninth VPI&SU Symposium on Dynamics and Control of Large Structures, Virginia Polytechnic Inst. and State Univ., Blacksburg, VA, 1993.

[6]Asada, H., and Slotine, J.-J. E., *Robot Analysis and Control*, Wiley, New York, 1986.

[7]Fanson, J. L., and Caughey, T. K., "Positive Position Feedback Control for Large Space Structures," *Proceedings of the AIAA/ASME/ASCE/AHS/ASC 28th Structures, Structural Dynamics, and Materials Conference* (Monterey, CA), AIAA, Washington, DC, 1989, pp. 588–598.

Low-Thrust Orbit Transfer Guidance Using an Inverse Dynamics Approach

Craig A. Kluever*
University of Missouri—Columbia/Kansas City, Kansas City, Missouri 64110

Introduction

MUCH research has been devoted to computing optimal low-thrust trajectories for solar electric propulsion (SEP) spacecraft. By comparison, the volume of work on guidance laws for electric propulsion spacecraft is somewhat limited. Trajectory optimization methods often utilize optimal control theory and the resulting Euler-Lagrange or costate equations define the thrust vector steering during the optimal transfer in an open-loop fashion. For realistic onboard guidance schemes, this technique is not feasible for the very long duration transfers performed by low-thrust spacecraft. Early studies on low-thrust guidance involved optimal neighboring control techniques[1,2] and nonoptimum, feasible schemes using reference trajectories.[3] Recently, a low-thrust guidance method using Lyapunov stability theory has been proposed.[4]

In this Note, a new guidance scheme using an inverse dynamics approach is developed for a general, three-dimensional, low-thrust transfer from circular low Earth orbit (LEO) to geosynchronous orbit (GEO). The goal is to devise an autonomous, reliable guidance scheme that computes the necessary thrust-direction steering for the LEO-GEO transfer and results in near-optimal performance. The guidance scheme utilizes the optimal, minimum-fuel transfer as a reference trajectory. Numerical results are presented for a typical SEP vehicle designed for a 200-day LEO-GEO mission.

Inverse Dynamics Guidance

The inverse dynamics guidance scheme is based on the optimal time histories of the semimajor axis a, eccentricity e, and inclination i. Therefore, the governing differential equations for these orbital elements are required. The equations of motion in an inverse-square gravity field for these orbital elements are

$$\frac{da}{dt} = \frac{2a^2 v}{\mu} a_T \cos\phi \cos\sigma \tag{1}$$

$$\frac{de}{dt} = \frac{a_T}{v}\left[2(e + \cos\nu)\cos\phi\cos\sigma + \frac{r}{a}\sin\nu\sin\phi\cos\sigma\right] \tag{2}$$

$$\frac{di}{dt} = \frac{r}{h}\cos(\omega + \nu) a_T \sin\sigma \tag{3}$$

In these equations, v is the velocity, r is the radial position, h is the angular momentum, ν is the true anomaly, ω is the argument of perigee, μ is the gravitational constant, a_T is the thrust acceleration, ϕ is the in-plane steering angle measured from the velocity vector to the projection of the thrust vector onto the orbit plane, and σ is the out-of-plane steering angle.

The guidance law is based on an inverse dynamics approach. Lu[5] recently presented an inverse dynamics approach to trajectory

Received Dec. 30, 1993; revision received March 29, 1994; accepted for publication April 19, 1994.

*Assistant Professor, Mechanical and Aerospace Engineering Department. Member AIAA.